การเปลี่ยนแปลงของปอดชั่วคราวที่พบในภาพรังสีทรวงอก ของผู้ป่วยติดเชื้อโควิด-19 ที่โรงพยาบาลสมเด็จพระยุพราชท่าบ่อ

อภิวิชญ์ กุดแถลง

กลุ่มงานรังสีวิทยา โรงพยาบาลสมเด็จพระยุพราชท่าบ่อ จังหวัดหนองคาย

Temporal Lung Changes in Chest X-Rays of COVID-19 Patients at Thabo Crown Prince Hospital

Apiwit Kudthalang

Department of Radiology, Thabo Crown Prince Hospital, Nong Khai, Thailand

บทคัดย่อ

หลักการและวัตถุประสงค์: โรคติดเชื้อไวรัสโคโรนา 2019 (โควิด-19) ซึ่งเป็นการระบาดใหญ่ทั่วโลก ถือเป็นโรคติดต่อร้ายแรงที่ทำให้เกิดการเปลี่ยนแปลงทาง พยาธิวิทยาของปอด ซึ่งอาจส่งผลให้เกิดภาวะปอดอักเสบรุนแรงจนถึงกลุ่มอาการหายใจลำบากเฉียบพลัน ในประเทศไทยการตรวจด้วยเครื่องเอกซเรย์เคลื่อนที่เป็น วิธีการที่ใช้กันแพร่หลายมากที่สุดในการประเมินและติดตามความผิดปกติของปอดในผู้ป่วยที่ติดเชื้อไวรัสโคโรนา 2019 การศึกษานี้มีจุดมุ่งหมายเพื่อศึกษาลักษณะ ภาพรังสีทรวงอกและการเปลี่ยนแปลงของปอดชั่วคราวที่พบในภาพรังสีทรวงอกของผู้ป่วยที่ติดเชื้อไวรัสโคโรนา 2019

วิธีการศึกษา: เป็นการศึกษาเชิงพรรณนาย้อนหลังของผู้ป่วยที่ติดเชื้อไวรัสโคโรนา 2019 ที่มีผลตรวจด้วยวิธี เรียลไทม์ พีซีอาร์ เป็นบวกที่เข้ารับการรักษาในโรงพยาบาล ตั้งแต่วันที่ 1 กรกฎาคม ถึง 31 สิงหาคม พ.ศ. 2564 ได้มีการเก็บข้อมูลประชากรของผู้ป่วยและทบทวนผลการตรวจเอ็กซ์เรย์ทรวงอก โดยที่ภาพรังสีทรวงอกแต่ละภาพ จะมีการให้คะแนนตามระดับความรุนแรงของรอยโรคในปอดในผู้ป่วยที่ติดเชื้อไวรัสโคโรนา 2019

ผลการศึกษา: ผู้ป่วยที่ติดเชื้อไวรัสโคโรนา 2019 ทั้งหมดจำนวน 487 ราย (เพศชายร้อยละ 48.3 และหญิงร้อยละ 51.7) อายุระหว่าง 3 เดือน ถึง 89 ปี (ค่าเฉลี่ย 36.22 ± 16.57 ปี) จำนวนภาพถ่ายรังสีทรวงอกผิดปกติที่นำมาวิเคราะห์จำนวน 335 รูปจากทั้งหมด 1,764 รูป (ร้อยละ 19) ความผิดปกติของภาพรังสีทรวงอก ที่พบมากที่สุดคือความผิดปกติชนิดเห็นเป็นฝ้าๆ กระจายในส่วนรอบนอกของปอดส่วนล่างทั้งสองข้าง ความผิดปกติชนิดนี้สามารถพัฒนาเป็นแบบหนาทึบที่กระจาย ในปอดสองข้างทั้งส่วนกลางและส่วนล่างได้ในช่วงประมาณวันที่ 1-9 โดยพบได้บ่อยสุดประมาณวันที่ 1-4 หลังจากเข้ารับการรักษาในโรงพยาบาล (แบบฝ้าๆ ร้อยละ 48, แบบหนาทึบ ร้อยละ 44) หลังจากนั้นความผิดปกติจะลดลงและเริ่มพบความผิดปกติแบบร่างแหประมาณวันที่ 10 หลังจากเข้ารับการรักษาในโรงพยาบาล ซึ่งเป็นลักษณะที่แสดงถึงการเริ่มระยะฟื้นฟูของโรค

สรุป: ภาพถ่ายรังสีทรวงอกมีประโยชน์ต่อการช่วยวินิจฉัย ประเมินและติดตามผู้ป่วยโรคปอดอักเสบจากการติดเชื้อไวรัสโคโรนา 2019 ระบบการให้คะแนนตามระดับ ความรุนแรงของรอยโรคในปอดเป็นวิธีที่ดีที่ใช้ในการพยากรณ์ความรุนแรงของโรคได้

คำสำคัญ: โควิด-19, โรคติดเชื้อไวรัสโคโรนา, ภาพถ่ายรังสีทรวงอก, ภาวะปอดอักเสบ

Abstract

Background and objective: Coronavirus disease 2019 (COVID-19), a novel worldwide pandemic, is a highly infectious disease, causing pathological lung changes that can result in severe pneumonia progressing to acute respiratory distress syndrome (ARDS). In Thailand, portable chest x-ray (CXR) machines are the most commonly used modality for assessment and follow-up of lung abnormalities in COVID-19 positive patients. This study aimed to describe CXR findings and temporal lung changes in COVID-19 patients.

Methods: A retrospective, descriptive study of patients with positive reverse transcription polymerase chain reaction (RT-PCR) tests for COVID-19 who were admitted from July 1 to August 31, 2021. Patients' demographics and CXR findings were reviewed. The lung finding scores were summed to produce a total severity score (TSS).

Results: A total of 487 patients were included in the study: male 48.3% and female 51.7%. The ages of the patients ranged from three months to 89 years with a mean of 36.22 ± 16.57 years. A total of 1,764 chest x-rays were obtained of the 487 patients. Three hundred and thirty-five baseline CXRs and the serial CXRs of 92 patients with abnormalities were analyzed to examine temporal lung changes. The most common findings from CXRs were peripheral ground-glass opacities (GGO) affecting the lower lung zones. In the course of illness, the GGOs progressed into consolidations affecting the middle and lower lung lobes at around 1-9 days, peaking at day 1-4 after the initial CXR (GGOs 48%, consolidations 44%). The consolidations regressed and reticulations were developed after day 10th from the initial CXR, indicating a healing phase.

Conclusion: Chest x-rays are good for assessing and monitoring patients with COVID-19 pneumonia; the CXR scoring system provided a good method to predict disease severity.

Keywords: COVID-19, coronavirus infections, chest x-ray, pneumonia

*Corresponding author: E-mail: Samantamorgan2310@gmail.com

Introduction

An outbreak of severe cases of pneumonia from an unidentified origin emerged in Wuhan, China on December 31, 2019.[1] The illness rapidly spread in China and many other countries. In January 2020, the World Health Organization (WHO) declared it a pandemic.[2] Coronavirus disease 2019 (COVID-19) emerged as an unprecedented health care and economic crisis. It is a highly infectious disease caused by severe acute respiratory syndrome coronavirus 2 (SARS-CoV-2).[3] At the time of writing (September 2021), there are more than 224 million confirmed COVID-19 cases and nearly 4.7 million deaths in over 200 countries around the world.[4] Since then, the number of cases is increasing day by day with no specific treatment.

In Thailand, the earliest case was reported in January 2020. COVID-19 has infected over 1.36 million patients in the country and continues to grow rapidly. COVID-19 infection caused by the novel coronavirus SARS-CoV-2 has been confirmed in many countries by real-time reverse transcription polymerase chain reaction (RT-PCR) tests on nasopharyngeal and throat swabs, with a positive rate of 30-70%.[5] Transmission by droplet and contaminated surfaces are believed to be the main modes of spread for SARS-CoV-2. The average incubation period is 14 days. Symptoms of the infection are variable and nonspecific. 50% of patients have no obvious symptoms. Commonly, patients present with fever, dry cough, fatigue, loss of smell, and loss of taste.[6]

Respiratory system involvement is common in COVID-19; that's why chest imaging plays a vital role in the diagnosis, risk stratification, and management of the patient. Several studies show that chest imaging can also be used in the diagnosis of COVID-19 as it helps to gauge the outcome for a patient by using some severity scoring methods.[6-8] Chest imaging is being routinely done in the form of a CXR and CT scan. Chest CT scans were found to be more sensitive than RT-PCR tests in confirming the diagnosis of COVID-19, reaching 98%.[7] Chest x-rays were found to have limited value in the initial diagnosis of COVID-19 with a sensitivity of about 69%.[8] Although chest-CT is more sensitive and specific than CXR, interpreting CXRs has always been a routine practice for clinicians to rule out other causes of respiratory disease. The lack of CT scans and radiologists, especially in developing countries such as Thailand, makes CXRs a great substitute for diagnosing and determining the severity and progression of lung abnormalities in COVID-19 patients, also taking into account that CXRs can be performed with portable equipment in isolation rooms. Such an option

also minimizes potential contact between patients and operators. The American College of Radiology notes that CT decontamination required after scanning patients with COVID-19 may disrupt radiological service availability and suggests that portable CXRs may be considered to minimize the risk of cross-infection.[8] However, images from portable machines are of poorer quality than those from a dedicated radiography facility, therefore can be more difficult to interpret.

Patients with COVID-19 had typical radiological findings from chest imaging including multifocal and bilateral ground-glass opacities and consolidations with peripheral and basal predominance. Septal thickening, bronchiectasis, pleural effusion, lymphadenopathy, and cavitation were less commonly seen.[4,7-9]

Information on CXR findings in patients with COVID-19 pneumonia is still limited in the literature and the majority of reports describe lung changes in chest CT scans.[3] For a better assessment of the findings on COVID-19 from portable CXR machines, this study aims to report CXR findings and describe temporal radiographic changes in patients with confirmed COVID-19 throughout the disease course. It is hoped that this study will enhance radiologists' and clinicians' understanding of CXR findings in COVID-19.

Materials and Methods

Study design

This is a retrospective descriptive study of laboratory confirmed COVID-19 patients who were admitted to the isolation wards of Thabo Crown Prince Hospital from July 1 to August 31, 2021. COVID-19 infection was confirmed by RT-PCR testing on nasopharyngeal swabs. Portable CXRs were performed at admission and followed up in all patients. All CXRs of COVID-19-confirmed patients were included in this study. A case record form was used to extract data from electronic medical records. Data collected included demographic characteristics, RT-PCR, and chest radiographic findings. The study was approved by the Institutional Ethical Committee. Written consent was waived by the ethics committee.

Image acquisition and analyses

All the chest x-rays were obtained as digital radiographs in the posteroanterior or anteroposterior projection using portable x-ray units in the isolation wards following the usual local protocols. Twenty-four of the initial CXRs were anteroposterior (24 of 487; 5%) and the rest were posteroanterior. One hundred and seventy-nine of the follow-up CXRs were anteroposterior (179 of 1,277;

14%), and the rest were posteroanterior. The CXRs were analyzed by one radiologist. The radiographic features were diagnosed according to the Fleischner Society glossary.[10] Ground glass opacity (GGO) was defined as an increase in opacification of the lung which does not obscure the blood vessels and airways. Consolidation was defined as a homogenous opacification that obscures the blood vessels and airway walls. Reticulation was defined as a collection of innumerable small opacities in a linear pattern. The presence of nodular opacity and pleural effusion were also recorded.

The distribution of lung lesions was categorized into: 1) right lung, left lung, or bilateral; 2) peripheral predominant, perihilar predominant, or diffuse. Demarcation was defined as half way between the lateral edge of the lung and the hilum; 3) zonal distribution: upper zone, middle zone, or lower zone. A severity score was determined for each lung using the Radiographic Assessment of Lung Edema (RALE) score proposed by Warren et al.[11] The score was determined by the involvement of each lung by consolidations or GGOs from 0 to 4 (0 = no involvement; 1 = < 25%; 2 = 25-50%; 3 = 50-75%; 4 = > 75% involvement). The scores for each lung were summed to produce the final severity score. Baseline and serial CXRs were reviewed and compared to determine if there were progression, stability, or improvement of lung changes over the time course of the illness. The series of follow-up CXRs were categorized according to the time of the initial CXR; CXR performed at baseline (initial CXR), 1-4 days, 5-9 days, 10-14 days, and over 15 days from the initial CXR (day 0).

Data analysis

Quantitative variables, such as age, were presented as mean along with the age range. Qualitative variables including gender and clinical outcomes were presented as frequency and percentages. The outcome variable, portable CXR findings, were presented as frequency and percentages. The data were tabulated and results were analyzed by using SPSS 24 software.

Results

Patients' characteristics

A total of 487 confirmed COVID-19 patients (by RT-PCR from nasopharyngeal swabs) were admitted to the hospital during the study period. There were 235 (48.3%) males and 252 (51.7%) females. Age of the patients ranged from 3 months to 89 years old with mean age was 36.22 ± 16.57 years. Table 1 shows patients' demographic characteristics and clinical outcomes.

Chest x-ray features

A total of 1,764 CXR were performed for 487 patients; 487 CXR at baseline and 1,277 CXR as follow-up. Baseline CXR were performed for all patients at the day of admission. Baseline CXR was normal in 416 patients (85.4%), while 43 patients (8.8%) and 28 patients (5.8%) had abnormal baseline CXR and indeterminate CXR, respectively. During follow-up CXR studies, 40 patients (8.2%) of the normal baseline CXR, as well as all patients (9; 1.8%) in the indeterminate group, showed CXR abnormalities. So CXR abnormalities were detected in 92 of 487 patients (18.9%) at certain points of the disease course (Table 2). Three hundred and ninety-five in 487 patients who tested positive for COVID-19 had negative CXR throughout their admission.

At baseline CXR (Table 3), ground-glass opacities (GGO) were the most common findings (35 of 43; 81.4%), followed by consolidations (8 of 43; 18.6%). Peripheral distribution (39 of 43; 90.7%), lower zone distribution (24 of 43; 55.8%) and bilateral involvement (24 of 43; 55.8%) were more common in locations and distributions. 38 patients (88.4%) had mild radiographic findings with total severity score of 1-2. More extensive involvement was observed in 4 (9.3%) and 1 (2.3%) patients, who had severity scores of 3-4 and 7, respectively.

Baseline CXR and serial CXR of 92 patients with abnormalities at certain points of the disease course (335 CXR; baseline CXR = 92 and serial CXR = 243) were performed and analyzed to see the course of the disease and temporal lung change. The baseline (initial) CXR at admission was recorded as day 0, the frequency of findings was as follow; GGO = 35/92 (38%), consolidations = 8/92 (8.7%), normal 40/92 (43.5%) and indeterminate 9/92 (9.8%). On serial follow-up CXR, GGO remained the most common lung abnormality pattern. At day 1-4 day from initial CXR, the frequency of the GGO was 41/86 (48%) and consolidations was 38/86 (44%). Two (2%) CXR were coarse reticulations and 5 (6%) CXR were normal. One patient with normal initial CXR (day 0), developed peribronchovascular consolidation in the right lower lung zone (right perihilar region/retrocardiac region) at day 4. One patient developed minimal right pleural effusion. The highest total chest radiography severity score (TSS) recorded was 8 at day 4.

At day 5-9, the frequency of CXR with GGO and consolidations decreased to 16/79 (20.3%) and 19/79 (24.1%), respectively. There was an increase in the number of mixed patterns; GGO/nodular and consolidations/reticulations (31/79; 39.2%) and reticulations in 6/79: 7.6%. The rest of CXR (7/79; 8.8%) were normal. The highest TSS recorded was 8 at day 5-7.

At day 10-14, the GGO and consolidations regressed (4/48; 8.3% and 5/48; 10.5%, respectively) but increased frequency of mixed pattern of nodular opacities, GGO,

and reticulations (24/48; 50%). Reticulations and normal CXR were also increased in frequencies in this phase comprising 6/48; 12.5% and 9/48; 18.8% of the CXR, respectively. The highest TSS recorded was 6.

After day 15, the number of consolidations was 3/30; 10%. The GGO and the mixed pattern regressed (2/30; 6.7% and 5/30; 16.6%, respectively). There was increase in the number and frequency of the reticulations (12/30; 40%). The normal CXR was 8/30; 26.7% in this group. The highest TSS recorded was 4. Figure 1 shows the distribution of CXR findings at different time intervals from initial CXR.

The spatial distribution of the radiographic lung changes was changed throughout the course of the disease during admission. Earlier in the disease (baseline/initial CXR), the lung abnormalities were seen predominantly in the periphery of the lungs, 39/92 (42.4%). Bilateral involvement was seen in 24/92 (26.1%). Unilateral involvement was seen in 8/92 (8.7%) on the right and 11/92 (12%) on the left. The lower zones were more frequently involved (21.7% right and 26.1% left).

At day 1-4 from initial CXR, the lung abnormalities extended from the periphery to the central giving much increase a diffuse pattern, from 2.2% (baseline CXR) to 46.7%. Bilateral involvement and lower zones involvement were noted in the majority of CXR. The numbers and percentage of the lower zones involvement and bilateral involvement were much increased (63.2% right lower zone, 74.6% left lower zone, and 50.4% bilateral). The middle zones were more frequently involved (12% to 58.8% right and 10.9% to 50.5% left). There was slightly increase in the frequency of right and left upper zone involvement (1.1% to 3.4% right and 1.1% to 2.8% left).

At day 5-9 from initial CXR, involvement of lower zones was predominant (60.7% right and 70.1% left). There was slightly increase in the frequency of right and left middle zones involvement (58.8% to 59.4% right and 50.5% to 57.1% left). Bilateral involvement and diffuse pattern were most common in this stage (66.6% and 50.4%). Increase frequency of right and left upper zone involvement was seen, from 3.6% to 5.4% and 2.8% to 7.2%, respectively.

At day 10-14 from initial CXR, bilateral lower zones were predominant (57.7% at the right and 60.4% at the left), reflecting slowly to recover. The frequency of right middle zone and left middle zone were 49.9% and 47.3%, respectively. Diffuse patterns were still predominant, 48.6%. A decrease in frequency of right and left upper zone involvement was seen; from 5.6% to 2.1% and 7.2% to 1.1%, respectively.

After 15 days from initial CXR, bilateral middle zones, bilateral lower zones, and isolated left lung disease were the last to recover (48.8% right middle, 51.3% right

lower, 52.4% left middle, and 56.6% left lower). Complete resolution of perihilar lesion, isolated right lung disease, and bilateral upper zones involvement was seen. Bilateral upper zones were the least to be involved throughout the course of the illness. Few patients had exclusive involvement of central/perihilar region of the lung with complete resolution. The frequency of normal CXR decreased from 43.5% at initial CXR to 6% at 1-4 days and 8.8% at 5-9 days, then increased to 18.8% at 10-14 days and 26.7% after 15 days as patients showed recovery. The specific frequencies of the spatial distribution of the temporal lung changes are in Figure 2.

The details of disease course and temporal lung changes throughout the study period in 92 patients who had radiographic abnormalities on CXR are as described; Three patients of indeterminate group progressed rapidly over an average period of 4 days seen as GGO and consolidations with increase TSS from 1-2 (day 1 from initial CXR) to 6-7 (day 3) and 8 (day 4). These patients showed gradual improvement from day 10-14 with regression of consolidations into GGO as well as development of some reticulations, which remained stable until day 14-18 (the end of the study) Figure 3.

Three patients of indeterminate group developed moderate findings on day 4 (TSS = 3-4), which showed partial improvement on serial follow-up CXR in day 5-8 (TTS = 1-2). Two patients of indeterminate group developed mild findings on day 2 (TSS = 2-3), which showed partial improvement on serial follow-up CXR in day 4-6 (TTS = 1-2). Two patients of indeterminate group developed moderate findings on day 4 (TSS = 3), which showed complete resolution on serial follow-up CXR in day 6-8. Four patients of indeterminate group developed moderate findings on day 3-4 (TSS = 4), which showed partial improvement on serial follow-up CXR in day 5 (TTS = 3). Two patients of indeterminate group developed mild findings (TTS = 2) with complete resolution in day 3-4. Three patients of indeterminate group developed mild findings (TTS = 1-2), which showed gradual improvement on serial follow-up CXR in day 5-8. At the end of the study, complete resolution was seen in 30 out of 92 patients who had initially mild disease (TTS = 1-2); 4 patients seen complete resolution at day 3-4, 12 patients in day 5-9, 8 patients in day 10-14 and 6 patients seen complete resolution over day 15.

Four patients who had initial chest radiography severity score = 4 with GGO showed developed consolidations in serial follow-up CXR day 1-4 with same chest radiography severity score then developed reticulations and GGO in day 6-8 (TTS decrease from 4 to 2). Four patients who had initial TSS = 2 with consolidations showed decrease in consolidation but developed reticulations on day 2-5 as well as residual reticulations on day 6-10 (TTS, decrease from 2 to 1). Three patients

who had initially severe disease with diffusely bilateral GGO and consolidations (TTS = 7-8) showed gradual improvement on serial follow up CXR day 6-8 with regressed consolidations and increase reticulations (TSS at day 6-8 and day 12; last film = 3-4). Three patients who had initially severe disease with diffusely bilateral consolidations (TTS = 7-8) showed gradual improvement on serial follow-up CXR day 6 with regressed consolidations and increase reticulations and GGO (TSS at day 6 and day 11; last film = 4). Five patients who had initially mild disease (GGO, TSS = 1-2) progressed to consolidations in day 4-8 (highest TSS = 5-8) then regressed as GGO and reticulations in day 10-14 (TSS = 2-3). Figure 4.

　　Five patients who had initially mild disease (GGO, TSS = 2) developed reticulations in day 5-8 with stable TSS. Four patients who had initially mild disease (small GGO and normal baseline CXR) showed radiological worsening on serial CXR day 1-4 and day 5-9 (the highest TSS were 6-8) then gradual improvement in day 10-14 (the highest TSS were 4-6) and interval static after day 14 until the end of the study. Three patients who had initially mild disease (bilateral peripheral GGO at middle and lower lung zones, TSS = 2-3) progressed to consolidations on day 2-4 (TSS = 4) then worsening on the daily serial CXR, the highest TSS = 6-8 at day 5-9. The abnormalities regressed as GGO, reticulations, and decrease lung volume on day 10 (TSS = 3). These findings were interval static in day 10-14. Four patients who had initial TTS = 3-4 with consolidations and GGO showed developed reticulations and GGO in day 2 serial CXR with same chest radiography severity score, 2 patients had gradual improvement on day 6 serial CXR (TSS = 2), 1 patient had gradual improvement on day 7 serial CXR (TSS = 2) and 1 patient had stable CXR until day 5 (last film). Four patients with normal baseline CXR developed abnormality on serial CXR, as follows; 2 patients developed GGO on day 2 (TSS = 2), progressed to consolidations on day 4 (TSS = 3) and developed reticulations on day 10 (TSS = 2), 2 patients developed GGO in day 8 serial CXR (TSS = 3-4) then regressed to reticulations in day 10-14 without complete resolution. Four patients with normal baseline CXR developed reticulations and a few tiny nodular opacities at peripheral middle and lower lung zones (TSS = 2-4) on day 6-10 CXR. There were 24 out of 92 patients who showed complete resolution of CXR abnormalities at over day 10 from initial CXR, which could be the absorption phase. The highest TSS recorded was 8 (the maximum possible score = 8). Peak severity score was reached at day 4-8 from initial CXR, representing the peak phase at which median TSS was 4.

Table 1 Patients' demographics, characteristics, and clinical outcomes (*n* = 487)

Characteristics	Number (%)
Sex	
Male	235 (48.3)
Female	252 (51.7)
Age (years), mean ± SD	36.22 ± 16.57
Clinical outcome at the end of the study	
Discharge	431 (88.5)
In admission	53 (10.9)
Died	3 (0.6)

Table 2 Distributions of baseline chest x-ray (*n* = 487)

Characteristic	Number (%)
Normal baseline CXR	416 (85.4)
Abnormal baseline CXR	43 (8.8)
Indeterminate baseline CXR	28 (5.8)
Patients with normal baseline CXR later becoming abnormal	40 (8.2)
Patients with indeterminate baseline CXR later becoming abnormal	9 (1.8)

Table 3 Radiographic findings and distribution on baseline chest x-ray in 43 patients

Parameter	Number (%)
Type of parenchymal opacity at CXR	
Ground-glass opacity	35 (81.4)
Consolidation	8 (18.6)
Distribution at CXR	
Peripheral predominant	39 (90.7)
Perihilar predominant	2 (4.7)
Diffuse	2 (4.7)
Right lung	8 (18.6)
Left lung	11 (25.6)
Bilateral lungs	24 (55.8)
Lobar involvement	
Right upper lung zone	1 (2.3)
Right middle lung zone	11 (25.6)
Right lower lung zone	20 (46.5)
Left upper lung zone	1 (2.3)
Left middle lung zone	10 (23.3)
Left lower lung zone	24 (55.8)

Discussion

In this pandemic, an accurate radiological approach is necessary for a more rapid classification of COVID-19 patients.[12,13] CXRs may not be as sensitive as CT scans, but they still play a major role in developing countries that lack more sophisticated modalities.[7] Moreover, CXR machines can be brought to the patient's bedside, minimizing the risk of cross-infection.[14-16] Based on the risks of misdiagnosis and viral transmission, the American College of Radiology (ACR) recommends that CT should not be used as a screening tool or as a first-line test to diagnose COVID-19. Instead, CT should be reserved for hospitalized, symptomatic patients with specific clinical indications.[8] Although CXRs have a low sensitivity to early-stage COVID-19, they can be used for monitoring the advancement and preceding stages of COVID-19, especially in critical care.[1,2,15-19,21,25] To provide valuable help for physicians and improve the stratification of the disease risk, the CXR scoring system was tailored to provide a semi-quantitative tool for assessment of lung abnormalities.[11]

In this study, every patient had at least one portable CXR done during their admission period. Pulmonary CT angiography (CTA) was performed on two patients with suspected pulmonary embolism. However, there was no definite evidence of pulmonary embolism in either patient. CXR abnormalities were detected in 92 of 487 patients (18.9%) proven to have COVID-19. The CXR abnormalities were analyzed for a course of the disease and temporal lung changes throughout their admission. The most common CXR findings in this study were GGO, followed by consolidations. These findings had peripheral distribution with bilateral lung involvement. There was lower lobes predilection of the opacities with the left lower lobe more common than the right lower lobe. These findings are in consensus with previous studies on CXR and CT scans.[18-22] The diffuse consolidations, as well as bilateral middle and lower zones involvements, progressed in one week after the initial CXR (day 1-8), and peaked at day 1-4 after the initial CXR. Consolidations were both new lesions and transformations from GGO. The TSS changed over time, reaching a peak at day 4-8 from the initial CXR. One patient showed peribronchovascular consolidation, which is not common in reports of COVID-19 pneumonia.[23,24] One patient had pleural effusion during this phase, which is not a common finding in chest imaging.[7,25] Phases of improvement of the CXR findings were seen in decreasing in size and extension of GGO/consolidations, the regression of consolidation into GGO, and reticulations which were seen over day 9 from the initial CXR. The bilateral middle zones, bilateral lower zones, and isolated left lung disease were the last to recover.

The peak and the absorption (improvement) phases in this study were seen to be earlier than the previous studies in 2020 (peak phase range at days 5-15 and absorption phase range at days 10-17).[14,19,26] Twenty-eight patients in the determinate group received a repeat CXR on the next day. One article mentioned features indistinguishable between equivocal/ unsure/ indeterminate for COVID-19 pneumonia and other cause (e.g., pseudolesion), required clinical correlation and short-interval follow up CXR.[27]

The major strength of this study was the evaluation of serial CXRs to examine the temporal radiographic changes. This study had several limitations. First, it was a retrospective study in which the recorded data included demographic characteristics and clinical presentations using the data from inpatient-outpatient medical records, and a database from the HOSxP program may be incomplete and inaccurate. Second, the lack of comparison between the scoring systems and patients' clinical condition (such as onset of symptoms, comorbidities, treatment). Third, the interval between the CXRs obtained was not uniform in all patients which may have led to undiagnosed abnormalities. Fourth, not all the patients could be followed till the final outcome or lack of long-term outcome. Fifth, for some severe cases, the portable CXR (especially anteroposterior CXR) was suboptimal viewing, causing limited evaluation.
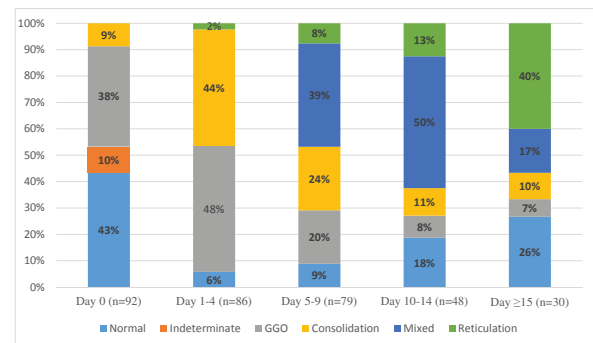

Figure 1 Temporal change of CXR findings. The Stacked-bar graph showed the distribution of the lung findings on CXR at various time points from initial CXR. GGO was the most frequent abnormality on initial CXR, consolidation increased in frequency till the first week then regressed on subsequent CXR. Mixed pattern of GGO and nodular consolidation and reticulations were gradually progressed in the second week. Normal CXR increased in frequency with time as patients showed radiological and clinical improvement. GGO = ground-glass opacity.
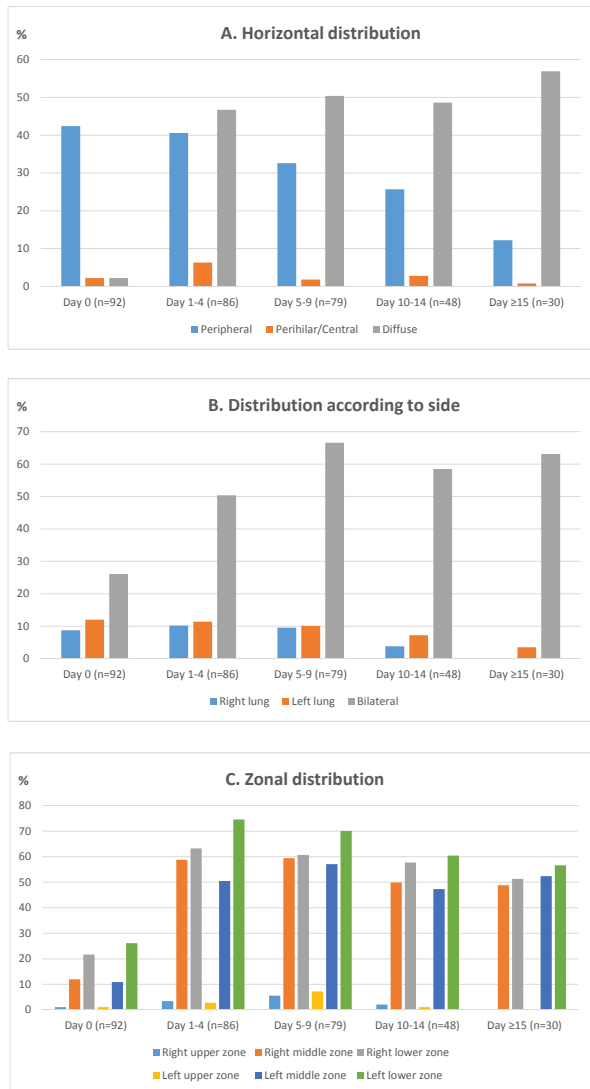
A. Horizontal distribution

B. Distribution according to side

C. Zonal distribution

Figure 2 The spatial distribution of the lung changes at various time intervals from symptom onset.

    A. Horizontal distribution. The lung changes were more frequently seen in a peripheral distribution on baseline/initial CXR, then developed to diffuse pattern on serial CXR.

    B. Distribution according to side. Bilateral distribution of the lung changes was more common than unilateral involvement on both baseline/initial CXR and serial CXR.

    C. Zonal distribution. Bilateral lower zones remained the most frequently involved over time, the upper zones were the least to be involved.
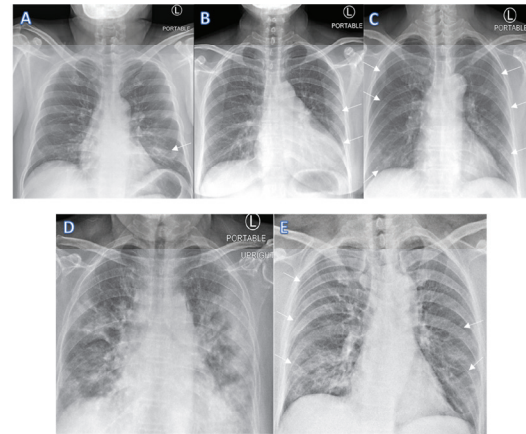

Figure 3 Series CXR in a 72 -year-old woman with positive COVID-19 virus.

    (A) An initial CXR showed subtle poorly defined opacities at left lower lung zone, indistinguishable between early/mild COVID-19 pneumonia or pseudolesion.

    (B) CXR obtained on day 1 showed peripheral GGO and consolidations at left middle and lower lung zones (TSS = 2, left 2 and right 0)

    (C) CXR obtained on day 3 showed diffuse consolidations extended to all lung zones except for perihilar regions (TSS = 6, right 3 and left 3)

    (D) CXR obtained on day 4 showed peaking of the findings with extensive diffuse patchy and nodular consolidations bilaterally (TSS = 8, right 4 and left 4).

    (E) CXR obtained on day 11 showed decrease in degree of lung involvement with reduction of overall TSS. There was regression of consolidations into GGO as well as development of reticulations at middle and lower zones, bilaterally (TSS = 5, right 3 and left 2).
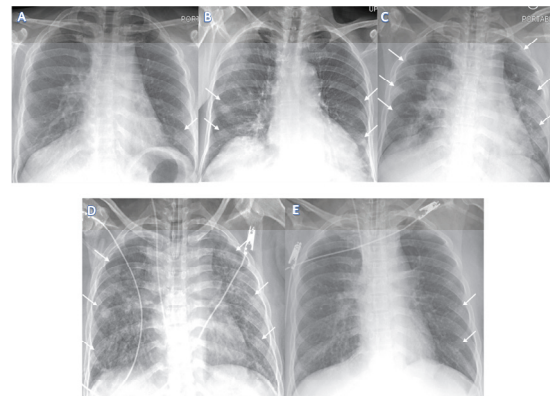

Figure 4 Series CXR in a 68-year-old man with positive COVID-19 virus.

    (A) An initial CXR showed small peripheral left lower zonal GGO with TSS = 1.

    (B) CXR obtained on day 3 showed increase in peripheral GGO at bilateral lower and middle zones (TSS = 4, right 2 and left 2).

    (C) CXR obtained on day 7 showed peaking of the findings with diffuse patchy consolidations mixed with GGO at both lungs (TSS = 7, right 4 and left 3).

    (D) CXR obtained on day 10 showed regression of consolidations into GGO and development of reticulations at both lungs (TSS = 6, right 3 and left 3).

    (E) CXR obtained on day 14 showed complete resolution of GGO with residual reticulations at left middle and lower zones (TSS = 2, right 0 and left 2).

Conclusions

About 18.9% of patients with confirmed COVID-19 had abnormal CXR findings. The most common findings on CXR were GGOs in a peripheral distribution with bilateral lower lobe predilection. The radiographic findings peaked at day 4-8 from the initial CXR, reaching the highest severity score and improved after day 9 from the initial CXR. The Radiographic Assessment of Lung Edema (RALE) score was used in this study with the addition of the bilateral middle zone involvement of COVID-19 as opposed to lower zone involvement alone. As mentioned previously, portable CXR was the most readily available and feasible investigation in our setups. This study showed that CXRs from a portable machine were good for assessing and monitoring patients with COVID-19 pneumonia and its scoring system provided a good method to predict the disease severity. Therefore, radiologists and clinicians can all benefit from this study.

References

1. World Health Organization. Novel coronavirus: China [Internet]. c2021 [cited May 1, 2021]. Available from: https://www.who.int/director-general/speeches/detail/who-director-general-s-opening-remarks-at-the-media-briefing-on-covid-19---11-march-2020

2. Salehi S, Abedi A, Balakrishnan S, Gholamrezanezhad A. Coronavirus disease 2019 (COVID-19): a systematic review of imaging findings in 919 patients. AJR 2020;215:1-7.

3. Kooraki S, Hosseiny M, Myers L, Gholamrezanezhad A. Coronavirus (COVID-19) outbreak: what the Department of Radiology Should Know. J Am Coll Radiol 2020;17:447–51.

4. Chung M, Bernheim A, Mei X, Zhang N, Huang M, Zeng X, et al. CT imaging features of 2019 novel coronavirus (2019-NCoV). Radiol 2020;295:202–7.

5. Sun P, Lu X, Xu C, Sun W, Pan B. Understanding of COVID–19 based on current evidence. J Med Virol: 1–4.

6. Feng W, Zong W, Wang F, Ju S. Severe acute respiratory syndrome coronavirus 2 (SARS-CoV-2): a review. Mol Cancer 2020;19(1):1-14.

7. Nasir MU, Roberts J, Muller NL, Macri F, Mohammed MF, Akhlaghpoor S, et al. The role of emergency radiology in COVID-19: from preparedness to diagnosis. Canadian Association of Radiol J 2020;71(3):293-300.

8. American College of Radiology. ACR recommendations for the use of chest radiography and computed tomography (CT) for suspected COVID-19 infection [Internet]. c2020 [update 2020 March 11; cited 2021 May 1]. Available from: https://www.acr.org/Advocacy-and-Economics/ACR-Position-Statements/Recommendations-for-Chest-Radiography-and-CT-for-Suspected-COVID19 Infection.

9. Cleverley J, Piper J, Jones MM. The role of chest radiography in confirming covid-19 pneumonia. BMJ 2020;370:242-6.

10. Hansell DM, Bankier AA, MacMahon H, McLoud TC, Müller NL, Remy J. Fleischner Society: glossary of terms for thoracic imaging. Radiol 2008;246(3):697-722.

11. Warren MA, Zhao Z, Koyama T, Bastarache JA, Shaver CM, Semler MW, et al. Severity scoring of lung oedema on the chest radiograph is associated with clinical outcomes in ARDS. Thorax 2018;73(9):840–6.

12. Toussie D, Voutsinas N, Finkelstein M, Cedillo MA, Manna S, Maron SZ, et al. Clinical and chest radiography features determine patient outcomes in young and middle-aged adults with COVID-19. Radiol 2020;297(1):197–206.

13. Meng H, Xiong R, He R. CT imaging and clinical course of asymptomatic cases with COVID-19 pneumonia at admission in Wuhan, China. J Inf Secur 2020;12:211–5.

14. Wong HYF, Lam HYS, Fong AHT. Frequency and distribution of chest radiographic findings in COVID-19 positive patients. Radiol 2019;27:201-6.

15. Jacobi A, Chung M, Bernheim A, Eber C. Portable chest X-ray in coronavirus disease-19 (COVID-19): a pictorial review. Clin Imaging 2020;64:35–42.

16. Borghesi A, Maroldi R. COVID-19 outbreak in Italy: experimental chest X-ray scoring system for quantifying and monitoring disease progression. Radiol Med 2020;125(5):509-13.

17. Yasin R, Gouda W. Chest X-ray findings monitoring COVID-19 disease course and severity. Egypt J Radiol Nucl Med 2020;51:193-7.

18. Rousan LA, Elobeid E, Karrar M, Khader Y. Chest x-ray findings and temporal lung changes in patients with COVID-19 pneumonia. BMC Pulm Med 2020;20(1): 245-53.

19. Kong W, Agarwal PP. Portable chest X-ray in coronavirus disease-19 (COVID-19): a pictorial review. Radiol Cardiothorac Imaging 2020;14:215-26.

20. Kanne JP. Chest CT findings in 2019 novel coronavirus (2019-nCoV) infections from Wuhan, China: key points for the radiologist. Radiol 2020;352:1791-98.

21. Wang D, Hu B, Hu C. Clinical characteristics of 138 hospitalized patients with 2019 novel coronavirus-infected pneumonia in Wuhan, China. JAMA 2020;35:664-70.

22. Pan F, Ye T, Sun P, Gui S, Liang B, Li L, et al. Time course of lung changes on chest CT during recovery from 2019 novel coronavirus (COVID-19) pneumonia. Radiol 2020;295(3):715–21.

23. Zhou S, Wang Y, Zhu T, Xia L. CT features of coronavirus disease 2019(COVID-19) pneumonia in 62 patients in Wuhan, China. AJR Am J Roentgenol 2020;214(6): 128-34.

24. Durrani M, Haq IU, Kalsoom U, Yousaf A. Chest X-ray findings in COVID 19 patients at a University Teaching Hospital - A descriptive study. Pak J Med Sci 2020;36:22-36.

25. Cozzi D, Albanesi M, Cavigli E. Chest X-ray in new Coronavirus Disease 2019 (COVID-19) infection: findings and correlation with clinical outcome. Radiol Medica 2020;125(8):730-7.

26. Wasilewski PG, Mruk B, Mazur S, Półtorak-Szymczak G, Sklinda K, Walecki J. COVID-19 severity scoring systems in radiological imaging – a review. Polish J Radiol 2020;85(1):361–8.

27. Thitiporn Suwatanapongched, Chayanin Nitiwarangkul, Warawut Sukkasem, Sith Phongkitkarun. A Guide to Classification of Abnormalities from Chest X-rays for the Diagnosis of Pneumonia in Patients with COVID-19 (Version 1). Bangkok : Department of Diagnostic and Therapeutic Radiology, Mahidol University, Faculty of Medicine Ramathibodi Hospital. 2021. [Cite May 1,2021]. Available from: https://med.mahidol.ac.th/radiology/sites/default/files/public/knowledge/20210505050251.pdf.

SMJ